VIII International Conference on Computational Methods for Coupled Problems in Science and Engineering
COUPLED PROBLEMS 2019
E. Oñate, M. Papadrakakis and B. Schrefler (Eds)

FLOW TOPOLOGY OPTIMIZATION IN PERIODIC DOMAINS WITH APPLICATION TO MICRO HEAT EXCHANGER OPTIMIZATION

A. Ghasemi* **and A. Elham†**

Technical University of Braunschweig
Hermann-Blenk-Str. 35, D-38108 Braunschweig, Germany

Key words: Topology optimization, Density–based, External flow, Micro heat–exchangers, Pseudo–spectral scheme

Abstract. The focus of this paper is topology optimization of fluid flow systems, particularly 2D laminar flows, widely found in microfluidic devices. The flow equations are solved numerically using a pseudo–spectral scheme and accurate derivatives are directly derived to facilitate gradient–based optimization. The proposed tool is utilized to enhance the performance of micro heat exchangers, in terms of minimizing the total pressure drop required to be supplied by micro pumps. It is well known that the geometry and arrangement of pinned fins play a pivotal role in total pressure drop of the system. Hence, in this work we aim to find the optimum topologies for various test cases by minimization of drag force on pined fins with a constraint on volume.

1 Introduction

Optimal design of flow systems is an important concern meanwhile a complex task, aiming performance enhancements. The accurate analysis of flow behavior is widely done using computational fluid dynamics (CFD) tools. Topology optimization (TO) [1] is a powerful approach towards finding the optimal systems. In contrast to shape optimization techniques, TO is free to modify topological features of a system to find the optimum design and ideally does not rely on initial designs. TO was initially developed for design of solid structures, and has been widely studied in the past decades (see [2]). A common TO approach is the so-called density-based method. In this approach material distribution is stated by design variables in space, ranging from 0 (empty) to 1 (full solid). Topology optimization in flow systems can be treated in a similar way: a continuous material function, ranging from 0 to 1, is used to define whether at a specific location the material

*e-mail: a.ghasemi@tu-braunschweig.de
†e-mail: a.elham@tu-braunschweig.de

is fluid, solid, or a porous material (solid with permeability) for the case of values between 0 and 1 [3].

TO of flow systems are widely studied, particularly for internal flow problems. For example, [4] studied steady channel flow case, [5] using the lattice Boltzmann method for TO of unsteady flow problems. More recently [6] developed a TO tool for turbulent flows. External flow TO studies are very limited in literature, possibly due to the deficiency of the conventional density-based approach, in which the pressure field is propagated through solid bodies [7]. External flow TO using density based methods are mainly developed in the basis of fluid–structure interaction (FSI) problems [8, 9] and [10].

In this work we present a TO tool developed to find the optimal topologies of pin fin type micro heat exchangers [11]. A common configuration of such devices is an array of cylindrical pins uniformly spread between two plates (see figure 1), in which fluid is pumped inside plates in order to increase the cooling performance.

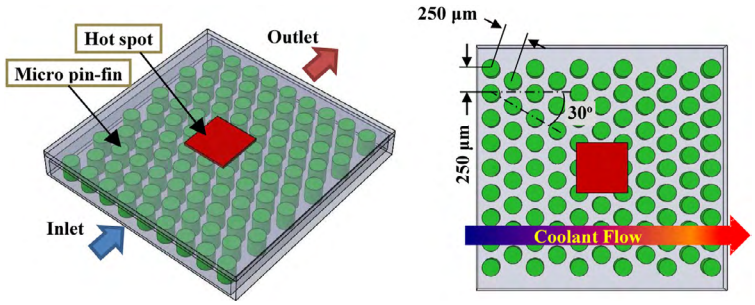

Figure 1: Schematic of a cylinderical micro pin fin heat exchanger (from [12]).

The performance of micro heat sinks is evaluated by first, maximum heat transfer rate and second, by the pressure drop [13] required to be supplied by micro pumps, which the latter is our prior concern in this paper. In this paper, we aim to find the optimal topologies of mico pin-fins with a volume constraint (cross section area) to minimize the pressure drop.

2 Governing equations

2.1 Fluid equation

Let us consider an incompressible and viscous fluid flow across a two dimensional and doubly periodic square domain, Ω, with neglected external forces. The flow is mathematically modeled using the time–dependent Navier–Stokes equations:

$$\frac{\partial \mathbf{u}}{\partial t} + \mathbf{u} \cdot \nabla \mathbf{u} + \frac{1}{\rho} \nabla P - \nu \Delta \mathbf{u} = 0 \tag{1}$$

and

$$\nabla \cdot \mathbf{u} = 0, \tag{2}$$

where $\mathbf{u}$ is the velocity vector, P is the hydrodynamic pressure, ν is the kinematic viscosity and ρ is the density of the fluid. Using the method of Brinkman penalization [14, 15], in order to define a material (solid or fluid) distribution, the equation 1 is modified such that the flow velocity in solid zones (Ω_s) is forced to become 0, i.e. no permeability into the solid material. Therefore, similar to what developed in [16], the penalized Navier–Stokes is formed as

$$\frac{\partial \mathbf{u}_\epsilon}{\partial t} + \mathbf{u}_\epsilon \cdot \nabla \mathbf{u}_\epsilon + \frac{1}{\rho}\nabla P - \nu \Delta \mathbf{u}_\epsilon - \frac{1}{\epsilon}\chi(\mathbf{x})\mathbf{u}_\epsilon = 0 \tag{3}$$

$$\nabla \cdot \mathbf{u}_\epsilon = 0 \tag{4}$$

where $\mathbf{u}_\epsilon$ is the approximated solution of equations (1) and (2) for fluid velocity, ϵ the penalization parameter which controls the flow permeability within solid zones and the dimensionless function $\chi(\mathbf{x})$ defines solid and fluid zones of the domain. $\chi(\mathbf{x})$ is set to 1 if $\mathbf{x} \in \Omega_s$ (solid bodies, Ω_s) and 0 otherwise (fluids). In [17] it is shown that the solution of penalized equations 3 and 4 converges to the solution of 1 and 2 wherein the error norm is bounded by

$$||\mathbf{u} - \mathbf{u}_\epsilon|| \leq C\,\epsilon^{1/4} \tag{5}$$

meaning smaller the ϵ, smaller the penalization error. However [17] reported $\epsilon^{1/2}$ as the upper bound on error norm based on numerical experiments. Penalization technique is suitable for topology optimization (density-based approach), because solid bodies are defined easily by modifying equations instead of modifying computational meshes. The corresponding boundary conditions in our case are defined as

$$\begin{cases} \mathbf{u} = 0 & \partial\Omega_s \\ \mathbf{u} \text{ is double periodic} & \text{on } \Omega, \end{cases} \tag{6}$$

and the mean flow velocity is $\mathbf{u}_\infty$ at upstream. The pressure term in equation 3 is eliminated by utilizing an orthogonal projector $\mathbb{P}$ onto the divergence–free space [18] for a space–periodic domain, which is based on Helmholtz decomposition providing a unique solution [19]. Equations 3 and 4 after projection become

$$\frac{\partial \mathbf{u}_\epsilon}{\partial t} + \mathbb{P}(\mathbf{u}_\epsilon \cdot \nabla \mathbf{u}_\epsilon) - \nu \Delta \mathbf{u}_\epsilon - \frac{1}{\epsilon}\chi(\mathbf{x})\mathbf{u}_\epsilon = 0, \tag{7}$$

where $\mathbb{P}$ is an orthogonal projector. In what follows, the ϵ subscription is removed for brevity.

2.2 Numerical method

In this work, the pseudo–spectral method presented by [16], is used to numerically approximate the solution of equation 7 by Fourier series; therefore, the 2–D flow velocity is approximated at point $\mathbf{x}$ and time t by

$$\mathbf{u}(x_1, x_2, t) = \sum_{k \in Z^2} \mathbf{u}_k(t) \exp\left[2\pi i \left(\tfrac{k_1 x_1 + k_2 x_2}{L}\right)\right] \tag{8}$$

where $x_1,\ x_2 \in]0\ L[$, in which L is the width or height of the physical domain, and k_1 and k_2 the wave numbers. The 2–d Fourier transform of equation 8 in the matrix form is simply performed by

$$\mathbf{U} = D\mathbf{U_k}D^T \tag{9}$$

where $\mathbf{U}$ and $\mathbf{U}_k$ are N-by-N matrices of the flow velocity u and u_k discretized in the physical and Fourier domain, respectively, and D the 2–D discrete Fourier transform matrix. In addition to the high spectral accuracy of the method, and the convenience of the spatial differentiations to be calculated in the Fourier space [20], the highly simple and well–structured form of the method allows a more convenient way of sensitivity analysis required for gradient based optimizations, in contrary to common flow numerical solving approaches, e.g. SIMPLE [21] in which the complexity and iterative nature of the solvers, discrete sensitivity analyses are rather much complex and error–prone. Discrete Fourier transform of 9 can be either easily parallelized for direct computations or computed using fast Fourier transform packages, e.g. FFTW [22]. The equation 7 after using a divergence–free projector $\mathbb{P}$, becomes

$$\frac{\partial \mathbf{u}}{\partial t} = \mathbf{u} \times \omega + \nu \Delta \mathbf{u} + \frac{1}{\epsilon}\chi(\mathbf{x})\mathbf{u} \doteq \mathbf{\Gamma}(\mathbf{u}, \chi(\mathbf{x})), \tag{10}$$

where ω is the flow vorticity. The projection is performed in the Fourier space and $\mathbb{P}$ is

$$\mathbb{P} = (k_1^2 + k_2^2)^{-1} \begin{bmatrix} k_2^2 & -k_1 k_2 \\ -k_1 k_2 & k_1^2 \end{bmatrix}. \tag{11}$$

3 Topology optimization

The general optimization problem we study in this paper is as follows:

$$\begin{aligned} \underset{\gamma}{\text{minimize}} \quad & C(\chi(\gamma),\, \mathbf{u}(\chi(\gamma))) \\ \text{subject to} \quad & V^* \leq V(\chi(\gamma)) \\ & 0 \leq \gamma_i \leq 1 \qquad \forall \gamma_i \in \Omega_D. \end{aligned} \tag{12}$$

where C is the objective function, which is particularly the drag force in this work, V is the volume (cross–section area) and γ is the vector of design variables. V^* is the minimum required volume, and the topology function χ is defined as a function of design variables, γ, using a continuous projection function as suggested in [23]:

$$\chi(\gamma) = \frac{\tanh(\beta\eta) + \tanh(\beta(\gamma - \eta))}{\tanh(\beta\eta) + \tanh(\beta(1 - \eta))}, \tag{13}$$

where, η and β are projection parameters which control sharpness of transition from solid to fluid by changing γ. In this paper, $\eta = 0.5$ and $\beta = \{1,\ 2,\ 4,\ 8,\ 16\}$, depending on the problem. It should be also noted that the gradients are updated using chain–rule since the derivatives are required to be with respect to the design variables γ.

As the optimization algorithm, the globally convergent method of moving asymptotes (GCMMA) [24] is used. This optimization algorithm is specially suited for problems with large number of design variables which is up to $\sim$ 3000 in our case. The optimizer is adjusted with the standard settings, but the step move parameter and the maximum number of sub-cycles limits are limited to 0.1 and 10, respectively.

3.1 Drag force

The drag force is the measure of the design to be minimized in this work and is simply calculated by integrating the Brinkman penalization term over the solid zones [14] as

$$\mathbf{F}_D = \frac{1}{\epsilon}\int_{\chi} \mathbf{u}\, \mathrm{d}\mathbf{x}. \tag{14}$$

It is noticeable that the drag force is accurately calculated at low cost [25] without the need for the knowledge of solid–fluid boundary, which is difficult to be tracked within the topology optimization process.

3.2 Sensitivity analysis

It is essential to provide an accurate sensitivity analysis of the flow system in order to take the gradient based optimization techniques. C (the drag force) using the equation 14 is as follows

$$C = C(u,\ v,\ \chi). \tag{15}$$

Therefore, the total derivative of C with respect to design variables, γ, using the chain rule is calculated by

$$\frac{DC}{D\gamma} = \frac{\partial C}{\partial \chi}\frac{\partial \chi}{\partial \gamma} + \frac{\partial C}{\partial u}\frac{Du}{D\chi}\frac{D\chi}{D\gamma} + \frac{\partial C}{\partial v}\frac{Dv}{D\chi}\frac{D\chi}{D\gamma}, \tag{16}$$

in which, the simplicity of equation 14 allows calculation of $\frac{\partial C}{\partial \chi}$, $\frac{\partial C}{\partial u}$ and $\frac{\partial C}{\partial v}$, at low cost and $\frac{D\chi}{D\gamma} = \frac{\partial \chi}{\partial \gamma}$ is simply derived from equation 13. The total derivatives $\frac{Du}{D\chi}$ and $\frac{Dv}{D\chi}$ are derived by taking the derivative of the discrete solution of equation 10. The solution of 10 at time step $n+1$, using Euler time integration scheme is

$$\begin{cases} u^{n+1} = u^n + \Delta \mathrm{t}\Gamma_u(u^n, v^n, \chi) \quad \text{and} \quad u^0 = u_{init} \\ v^{n+1} = v^n + \Delta \mathrm{t}\Gamma_v(u^n, v^n, \chi) \quad \text{and} \quad v^0 = v_{init}, \end{cases} \tag{17}$$

where Δt is the time step size, chosen based on CFL condition for numerical stability. By taking the derivative of equations 17 with respect to χ, we derive

$$\begin{cases} \frac{Du}{D\chi}^{n+1} = \frac{Du}{D\chi}^{n} + \Delta \mathrm{t}\,[\frac{\partial \Gamma_u}{\partial \chi} + \frac{\partial \Gamma_u}{\partial u}\frac{Du}{D\chi} + \frac{\partial \Gamma_u}{\partial v}\frac{Dv}{D\chi}]^n \quad \text{and} \quad \frac{Du}{D\chi}^{0} = 0 \\ \frac{Dv}{D\chi}^{n+1} = \frac{Dv}{D\chi}^{n} + \Delta \mathrm{t}\,[\frac{\partial \Gamma_v}{\partial \chi} + \frac{\partial \Gamma_v}{\partial u}\frac{Du}{D\chi} + \frac{\partial \Gamma_v}{\partial v}\frac{Dv}{D\chi}]^n \quad \text{and} \quad \frac{Dv}{D\chi}^{0} = 0, \end{cases} \tag{18}$$

where the the partial derivatives for Γ_u and Γ_v, could be assembled once for each geometry using the converged solution of equations 17. Since the flow is laminar and steady–state (for relatively low Reynolds numbers), after sufficiently large number of steps, $\frac{Du}{D\chi}^n$ and $\frac{Dv}{D\chi}^n$ are converged; hence, the total derivative of equation 16 is calculated. Deriving sensitivities are iterative in this approach but rather fast since the information from previous optimization steps are used as the initial values of the derivatives. This method is simply parallelization and accurate, and no specific strategy, e.g. automatic differentiation (AD) [26] is used. The sensitivities accuracies are controlled by convergence tolerance and are validated using finite differencing method.

4 Topology optimization of micro heat exchangers

In this section we focus on three optimization cases for the design and configuration of pin–fin micro heat exchangers, aiming to minimize the drag. In the first case, we start the optimization process with an initial design which is commonly used for such micro–fluidic devices: an array of cylinders. In the second case, in contrary to the first case, we initiate the optimization from nothing, i.e. no initial solid zones are set initially. This test case examines the capability our numerical approach in terms of providing a flexible and robust design tool for external flow topology optimization problems. And lastly, similar to the first case, we attempt finding an optimized topology and initially start from a cylinder array; however, we fix the initial design during the optimization. The first two cases are constrained optimizations problems by defining a minimum volume to be shaped in the final design and the last case is unconstrained, i.e. the optimizer is free to add solid parts throughout the design domain.

Figure (2) shows the simulation setup. The Reynolds number is fixed to 25, common value for micro scale fluidic devises with steady laminar flows, based on the unit length scale ($L_{ref} = 1$) of the reference domain (Ω_{ref}). Flow simulation domain (Ω) has a fixed size of $L = 2$, based on pitch-to-diameter ratio $L/L_{ref} = 2$ configuration, however the design domain ($\Omega_D \subseteq \Omega$) is defined for each case, separately. The mean upstream flow velocity is considered $\mathbf{u}_{up} = 2$ with two angles: 0 (in–line) and $\pi/4$ (staggered). Penalization parameter is $\epsilon = 0.005$ which demonstrates nearly impermeable solid. The

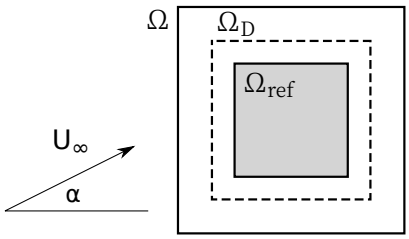

Figure 2: Schematic illustration of flow, design and reference domain.

physical domain is discretized by 64×64 points and simulations are computed on the

Test case	Initial C_D	Final C_D	Change (%)
#1: In-line	2.2093	1.3675	−38.1%
#1: Staggered	3.6466	2.2324	−38.8%

Table 1: Drag and drag reduction for case 1.

Phoenix cluster of TU Braunschweig [12] in parallel. The volume (cross section area) is defined by summation of χ_i's over Ω_s and the drag coefficient C_D for a better comparison, similar to Reynolds number, is calculated based on fixed upstream flow velocity and the unit length of the reference domain (Ω_{ref}), for all cases.

4.1 Case 1: minimum drag from an initial design

Any topology optimization tool essentially is required to be able to optimize shapes as well. In this setting, we aim to examine the present optimization framework. In this example we investigate the optimal heat exchanger topologies, in terms of minimum pressure drop, starting from an initial configuration: a cylinder array. We seek for a design which satisfies the minimum volume constraint equivalent to the initial cylinder. Figure (3) illustrates the initial and final topologies within the fluid flow. In (3a) and (3c), we observe larger wake areas where the flow velocity is close to zero, and consequently larger flow acceleration in gaps between cylinders. However, in (3b) and (3d) the final optimum topologies feature reduced cross–flow area, and hence, reduced the wake areas with the same volume. As listed in table (1), we see the new geometries have successfully reduced the drag force considerably, both for in-line and staggered configurations. In (3b), due to the jet-like format of flow structure, the optimum topology has nearly maximum aspect ratio while preserving a topology with aerodynamically shaped geometry. Therefore we observe the final optimum is spanned throughout Ω_D. In staggered case, the flow velocity direction and magnitude is changed frequently. In (3d), we observe the new topology has eliminated most of the wake region in (3c) and flow is well directed with less maximum flow velocity due to the larger gap space in between. It should be noted that the final topologies and the drag reductions listed in table 1 are well in agreement with the numerical experiments performed by [12].

4.2 Case 2: minimum drag from zero initial solid volume

In this example, we try to find the optimum topologies initially from zero sold volume. It is an ideal feature of a topology optimization tool that is capable of creating topologies from nothing and here we aim to investigate this item. We restart examples in (4.1) with the same constraints on volume; hence, the optimizer begins with an infeasible starting inputs. As shown in (4), we observe topologies successfully similar to the case 1. This observation is approved also by comparing the drag values in table (2), where the drag

https://www.tu-braunschweig.de/it/dienste/21/phoenix

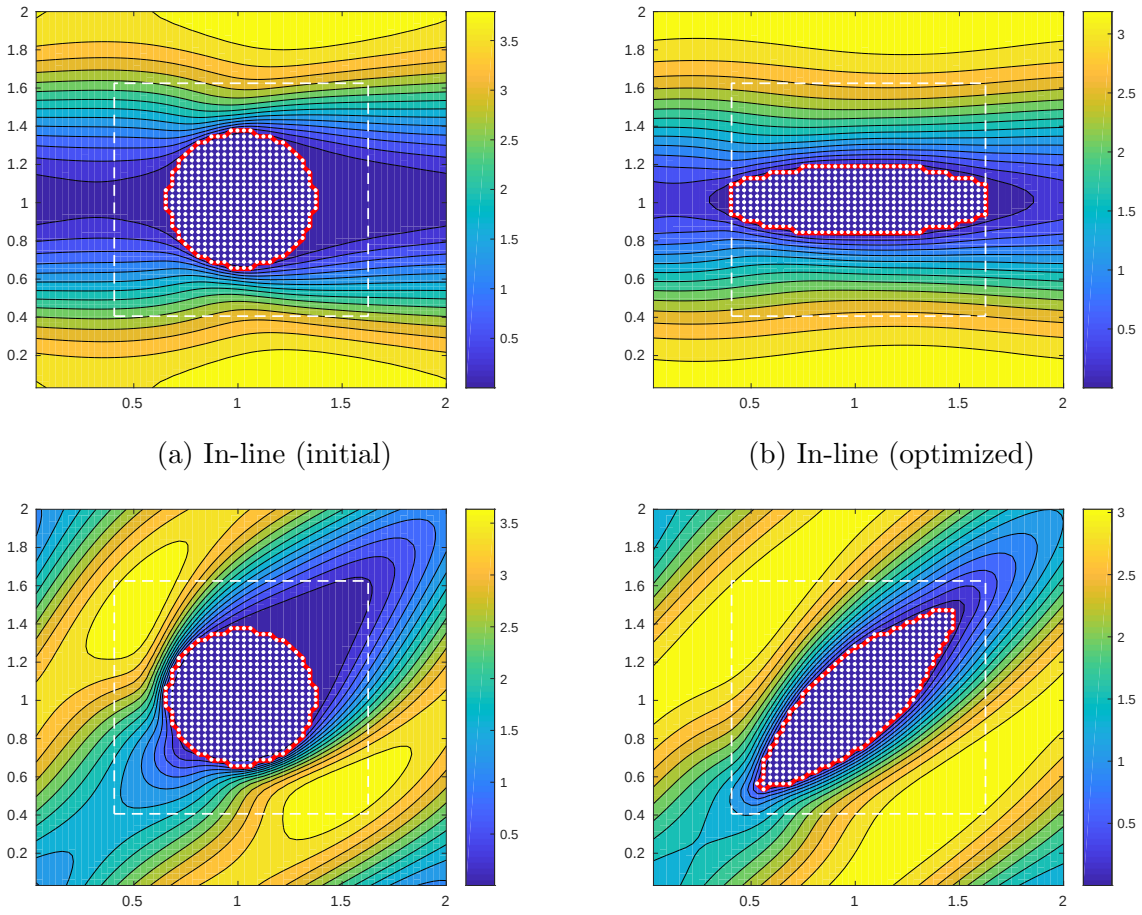

(a) In-line (initial)

(b) In-line (optimized)

(c) Staggered (initial)

(d) Staggered (optimized)

Figure 3: Illustration of flow velocity (magnitude) contours and solid geometries. The red line is the border of solid–fluid and white points are the nodal points corresponding to penalization zone (Ω_s).

forces are close to the case 1. This is a considerable achievements and brings insight to develop a more generalized flow topology optimization framework.

4.3 Case 3: drag minimization for a fixed design

Based on the promising performance of the present topology optimization approach, we aim to improve the initial design by performing an unconstraint optimization. In this case, we consider in-line and staggered cylinder arrays similar to part 4.1, but increased the initial volume. We choose a rather large design domain in order to give sufficient freedom to the optimizer to seek the best design. For this case, GCMMA parameters require adjustments, otherwise no meaningful results are achieved, and we used $\eta = 0.5$

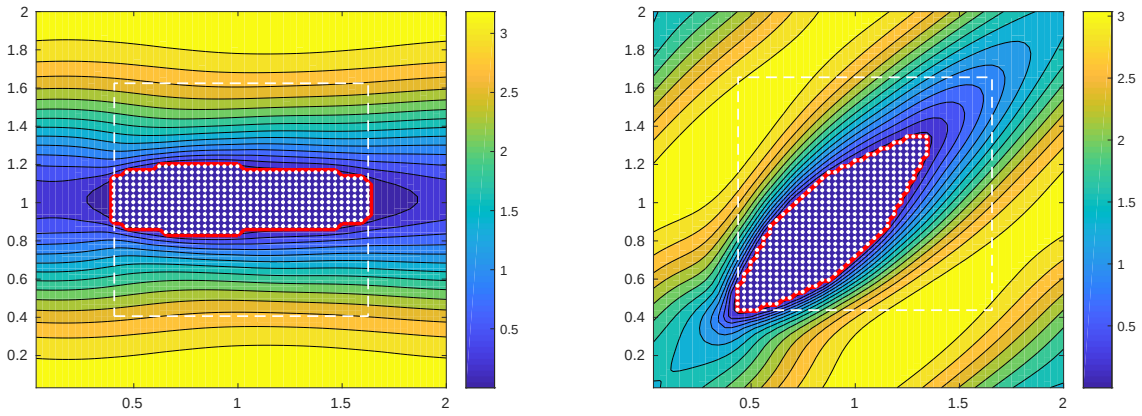

(a) In-line (optimized)

(b) Staggered (optimized)

Figure 4: Illustration of solid topologies designed from zero solid volume and contours of flow velocity magnitude.

Test case	Initial C_D	Final C_D	Compared to case 1
#2: In-line	0.0	1.3689	+1.543%
#2: Staggered	0.0	2.2434	+0.098%

Table 2: Drag force for case 2 compared to case 1.

and $\beta = 16$ for projection. The design domain is split into two parts: first, passive nodes inside the initial design to be unchanged within the optimization process and second, the active nodes to be either solid or fluid at the end.

The test cases are shown in figure 5. The enhanced topologies are noticeable in the sense that the optimization tool is well aware of the flow structure supported by accurate sensitivity analysis throughout the design domain. Both stream–wise fore-end and back-end of the cylinders are touched by the optimizer, in order to better guide the flow. In (5a), the wake is more intensive because the flow at up-stream is the wake region of the front cylinder. Hence, the added solid zones are wisely placed such that this area is filled and the aspect ratio is increased as we expect for a better aerodynamic performance. In (5b), a sharp element is added in the tip of the cylinder which improves the flow guidance and removes stagnation of fluid. At the tip, we observe a meaningful solid structure is merged to the cylinder which tends to minimize wake effect by elimination of flow circulations. Overall, as reported in table (3), the drag reductions are $\sim 1\%$ which are expectable because the flow is laminar without unsteady flow separation, in which the flow behavior at wake region and the boundary layer are more important. However, in the present test case, our topology optimization approach again demonstrated a great performance in terms of robustness, flexibility and accuracy. It is worth noting that the present optimization process requires considerably low iterations since in some cased we

Test case	Initial C_D	Final C_D	Change (%)	Initial V/V_{ref}	Final V/V_{ref}
#3: In-line	4.2274	4.1979	-0.697%	0.793	0.859
#3: Staggered	6.7451	6.7058	-0.581%	0.793	1.051

Table 3: Drag reduction for case 3.

reached to the optimum topology with less than ~ 50 iterations.

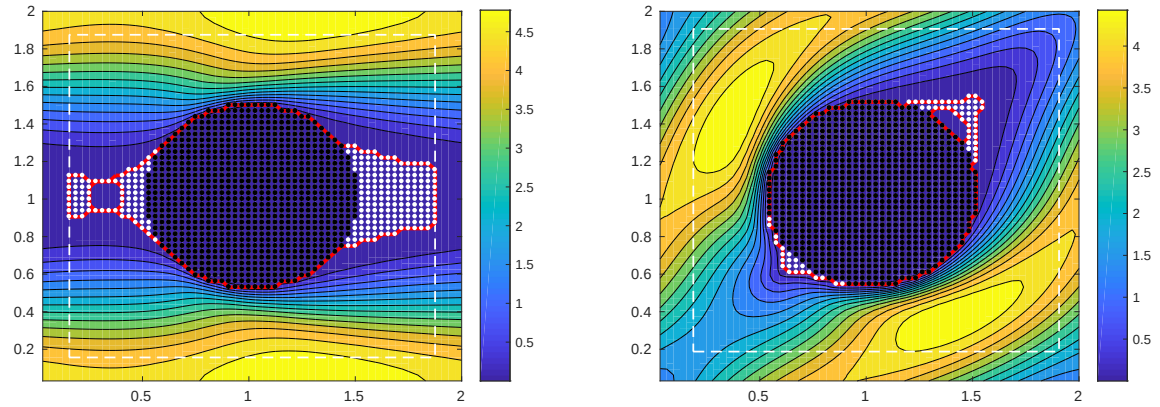

(a) In-line (optimized)

(b) Staggered (optimized)

Figure 5: Contours of flow magnitude and optimized topologies for in-line and staggered configurations. Black dots are passive nodes and white dots active nodes. The red-line represents again the solid-fluid boundary.

5 Conclusion

A new topology optimization tool has been developed for flow systems with incompressible laminar 2D flows in a doubly periodic domain. Using pseudo–spectral scheme and accurate sensitivity calculation, we attempted to minimize the drag force on each fin by optimizing the topology of pin–fin micro heat–exchanger. The total drag forces were successfully reduced by $\sim 38\%$ in both in–line and rotated configurations with the optimum topologies in agreement with the literature. In addition, we found that a noticeable feature of the present tool is the ability to find optimal topologies without providing an initial design for the optimization process, with final topologies well consistent with the initial case. Finally, we optimized topology of the cylindrical pin–fin geometries by limiting the optimizer to only adding material to the initial design. We observed that our topology optimization approach were able to successfully create meaningful topologies although due to the flow physics the drag reduction was limited to $\sim 1\%$.

REFERENCES

[1] Bendsoe, M. P. and Sigmund, Ole. *Topology Optimization: Theory, Methods and Applications*. Springer, 2004.

[2] Sigmund, Ole, and Kurt Maute. *Topology optimization approaches.* Structural and Multidisciplinary Optimization 48.6 (2013): 1031-1055.

[3] Borrvall, Thomas, and Joakim Petersson. *Topology optimization of fluids in Stokes flow*. International journal for numerical methods in fluids 41.1 (2003): 77-107.

[4] Gersborg-Hansen, Allan, Ole Sigmund, and Robert B. Haber. *Topology optimization of channel flow problems*. Structural and Multidisciplinary Optimization 30.3 (2005): 181-192.

[5] Nrgaard, Sebastian, Ole Sigmund, and Boyan Lazarov. *Topology optimization of unsteady flow problems using the lattice Boltzmann method*. Journal of Computational Physics 307 (2016): 291-307.

[6] Dilgen, Cetin B., et al. *Topology optimization of turbulent flows*. Computer Methods in Applied Mechanics and Engineering 331 (2018): 363-393.

[7] Kreissl, Sebastian, Georg Pingen, and Kurt Maute. *An explicit level set approach for generalized shape optimization of fluids with the lattice Boltzmann method*. International Journal for Numerical Methods in Fluids 65.5 (2011): 496-519.

[8] Yoon, Gil Ho. *Topology optimization for stationary fluid–structure interaction problems using a new monolithic formulation*. International journal for numerical methods in engineering 82.5 (2010): 591-616.

[9] Lundgaard, Christian, et al. *Revisiting density-based topology optimization for fluid-structure-interaction problems*. Structural and Multidisciplinary Optimization 58.3 (2018): 969-995.

[10] Kondoh, Tsuguo, Tadayoshi Matsumori, and Atsushi Kawamoto. *Drag minimization and lift maximization in laminar flows via topology optimization employing simple objective function expressions based on body force integration*. Structural and Multidisciplinary Optimization 45.5 (2012): 693-701.

[11] Tuckerman, David B., and Roger Fabian W. Pease. *High-performance heat sinking for VLSI*. IEEE Electron device letters 2.5 (1981): 126-129.

[12] Abdoli, Abas, Gianni Jimenez, and George S. Dulikravich. *Thermo-fluid analysis of micro pin-fin array cooling configurations for high heat fluxes with a hot spot*. International Journal of Thermal Sciences 90 (2015): 290-297.

[13] Siu-Ho, Abel, Weilin Qu, and Frank Pfefferkorn. *Experimental study of pressure drop and heat transfer in a single-phase micropin-fin heat sink.* Journal of Electronic Packaging 129.4 (2007): 479-487.

[14] Angot, Philippe, Charles-Henri Bruneau, and Pierre Fabrie. *A penalization method to take into account obstacles in incompressible viscous flows.* Numerische Mathematik 81.4 (1999): 497-520.

[15] Arquis, E., and J. P. Caltagirone. *Sur les conditions hydrodynamiques au voisinage dune interface milieu fluide-milieu poreux: applicationa la convection naturelle.* CR Acad. Sci. Paris II 299 (1984): 1-4.

[16] Kevlahan, Nicholas K-R., and Jean-Michel Ghidaglia. *Computation of turbulent flow past an array of cylinders using a spectral method with Brinkman penalization.* European Journal of Mechanics-B/Fluids 20.3 (2001): 333-350.

[17] Carbou, Gilles, and Pierre Fabrie. *Boundary layer for a penalization method for viscous incompressible flow.* Advances in Differential equations 8.12 (2003): 1453-1480.

[18] Deriaz, Erwan, and Valerie Perrier. *Direct numerical simulation of turbulence using divergence-free wavelets.* Multiscale Modeling & Simulation 7.3 (2008): 1101-1129.

[19] Foias, Ciprian, et al. *Navier-Stokes equations and turbulence.* Vol. 83. Cambridge University Press, 2001.

[20] Trefethen, Lloyd N. *Spectral methods in MATLAB.* Vol. 10. Siam, 2000.

[21] Patankar, Suhas. *Numerical heat transfer and fluid flow.* CRC press, 1980.

[22] Frigo, Matteo. *A fast Fourier transform compiler.* Acm sigplan notices. Vol. 34. No. 5. ACM, 1999.

[23] Wang, Fengwen, Boyan Stefanov Lazarov, and Ole Sigmund. *On projection methods, convergence and robust formulations in topology optimization.* Structural and Multidisciplinary Optimization 43.6 (2011): 767-784.

[24] Svanberg, Krister. *A globally convergent version of MMA without linesearch.* Proceedings of the first world congress of structural and multidisciplinary optimization. Vol. 28. Goslar, Germany, 1995.

[25] Kevlahan, NK-R., and J. Wadsley. *Suppression of three-dimensional flow instabilities in tube bundles.* Journal of fluids and structures 20.4 (2005): 611-620.

[26] Griewank, Andreas. *On automatic differentiation.* Mathematical Programming: recent developments and applications 6.6 (1989): 83-107.